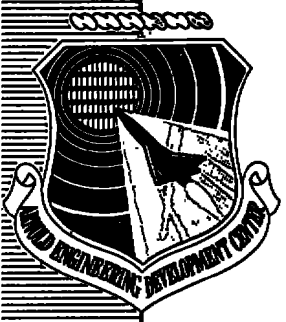

SHOCK-FITTING FOR FULL POTENTIAL EQUATION

M. M. Hafez and E. M. Murman

Flow Research Company
A Division of Flow Industries, Inc.
Kent, Washington 98031

December 1978

Final Report for Period January 1976 — April 1978

Prepared for

ARNOLD ENGINEERING DEVELOPMENT CENTER/DOTR
ARNOLD AIR FORCE STATION, TENNESSEE 37389

NOTICES

When U. S. Government drawings, specifications, or other data are used for any purpose other than a definitely related Government procurement operation, the Government thereby incurs no responsibility nor any obligation whatsoever, and the fact that the Government may have formulated, furnished, or in any way supplied the said drawings, specifications, or other data, is not to be regarded by implication or otherwise, or in any manner licensing the holder or any other person or corporation, or conveying any rights or permission to manufacture, use, or sell any patented invention that may in any way be related thereto.

Qualified users may obtain copies of this report from the Defense Documentation Center.

References to named commerical products in this report are not to be considered in any sense as an indorsement of the product by the United States Air Force or the Government.

This final report was submitted by Flow Research Company, a Division of Flow Industries, Inc., P. O. Box 5040, Kent, Washington 98031, under contract F40600-76-C-0007, with the Arnold Engineering Development Center/DOTR, Arnold Air Force Station, Tennessee 37389. Captain Stephen L. Lamkin, AEDC/DOTR, was the Air Force Technical Monitor.

This report has been reviewed by the Information Office (OI) and is releasable to the National Technical Information Service (NTIS). At NTIS, it will be available to the general public, including foreign nations.

APPROVAL STATEMENT

This report has been reviewed and approved.

Stephen L. Lamkin

STEPHEN L. LAMKIN, Captain, USAF
Project Manager, Research Division
Directorate of Test Engineering

Approved for publication:

FOR THE COMMANDER

Robert W. Crossley

ROBERT W. CROSSLEY, Lt Colonel, USAF
Acting Director of Test Engineering
Deputy for Operations

REPORT DOCUMENTATION PAGE	READ INSTRUCTIONS BEFORE COMPLETING FORM
1. REPORT NUMBER: AEDC-TR-78-37	2. GOVT ACCESSION NO. / 3. RECIPIENT'S CATALOG NUMBER
4. TITLE (and Subtitle): SHOCK-FITTING FOR FULL POTENTIAL EQUATION	5. TYPE OF REPORT & PERIOD COVERED: Final Report - January 1976 - April 1978
	6. PERFORMING ORG. REPORT NUMBER: Flow Research Note 142
7. AUTHOR(s): M. M. Hafez and E. M. Murman	8. CONTRACT OR GRANT NUMBER(s): F40600-76-C-0007
9. PERFORMING ORGANIZATION NAME AND ADDRESS: Flow Research Company, P. O. Box 5040, Kent, Washington 98031	10. PROGRAM ELEMENT, PROJECT, TASK AREA & WORK UNIT NUMBERS: Program Element 65807F
11. CONTROLLING OFFICE NAME AND ADDRESS: Arnold Engineering Development Center/OIS, Air Force Systems Command, Arnold Air Force Station, Tennessee 37389	12. REPORT DATE: December 1978
	13. NUMBER OF PAGES: 39
14. MONITORING AGENCY NAME & ADDRESS(if different from Controlling Office)	15. SECURITY CLASS. (of this report): UNCLASSIFIED
	15a. DECLASSIFICATION/DOWNGRADING SCHEDULE: N/A

16. DISTRIBUTION STATEMENT (of this Report)

Approved for public release; distribution unlimited.

17. DISTRIBUTION STATEMENT (of the abstract entered in Block 20, if different from Report)

18. SUPPLEMENTARY NOTES

Available in DDC

19. KEY WORDS (Continue on reverse side if necessary and identify by block number)

shock waves
algorithm
computations
shock-fitting
transonic flow
axisymmetric
bodies

20. ABSTRACT (Continue on reverse side if necessary and identify by block number)

In this report a procedure is considered for fitting shock waves in transonic type-dependent finite-difference relaxation calculations by using the full potential equation. The iterative line relaxation method for transonic finite-difference (rotated or conservative schemes) calculations can be described by a time-dependent equation. The shock-fitting algorithm presented here depends on this unsteady equation. Written in conservative form, the jump condition is derived in terms of shock speed. In the steady-state

20. ABSTRACT (Continued)

limit, shock speed vanishes, and the steady shock polar is retained. In this way the jump conditions are imposed iteratively and in a manner consistent with the relaxation procedure that is used everywhere else in the flow field. Preliminary results for axisymmetric flows around a sphere are presented. Application of the algorithm to small-disturbance calculations are discussed in the appendix.

PREFACE

The effort described in this report was conducted at Flow Research Incorporated, Kent, Washington, during the period January 1976 through April 1978. The work was accomplished under Air Force Contract F40600-76-C-0007 funded by the Research Division, Deputy for Operations, Arnold Engineering Development Center. Technical monitor was Captain Stephen L. Lamkin, AEDC/DOTR.

The reproducibles used in the reproduction of this report were supplied by the authors, Earll M. Murman and Mohammed Hafez.

The authors would like to thank Professor Anthony Jameson of Courant Institute for an interesting discussion on this subject. In addition, we thank B. Bell and P. McCafferty of Flow Research Company for their help with the calculations of the numerical examples. This research was supported by the Arnold Engineering Development Center under Contract No. F40600-76-C-0007.

CONTENTS

ILLUSTRATIONS

1. Introduction

In the past, transonic flows have been calculated with the Euler equations and with time-dependent finite-difference methods. For example, Magnus and Yoshihara[1] used the Lax-Wendroff finite-difference schemes with additional artificial viscosity. In their work, the shocks were smeared, and small grid sizes were needed to capture them. Grossman and Moretti,[2] on the other hand, fitted the shock following a method developed by Kentzer,[3] which uses the compatibility relations along the characteristics.

For many cases of interest, a potential flow model is adequate. Murman and Cole[4] introduced a type-dependent finite-difference scheme and solved the transonic small-disturbance equation by relaxation methods. Jameson,[5] using "rotated difference schemes," extended their work to the full potential equation. In their calculations, shock jump conditions are not satisfied. For example, mass is not conserved across the shock, and the strength and position of the shock are usually not calculated correctly. Later, Murman[6] introduced a "fully conservative scheme" to handle this problem for small-disturbance calculations, and Jameson[7] introduced a fully conservative scheme for the full potential equation. In these later calculations, mass is conserved globally, supersonic to subsonic shocks are located within a few grid points, and supersonic to supersonic shocks are usually smeared over more grid points. Sharper shocks can be obtained only by grid refinement.

Hafez and Cheng[8] considered shock fitting for transonic small-disturbance calculations by using type-dependent finite-difference relaxation methods. In their work, shock-jump conditions are explicitly imposed, and mass is locally conserved across a surface of discontinuity. Much coarser grids may then be used for the calculations. The algorithm applies for supersonic to subsonic shocks as well as for supersonic to supersonic shocks. Using characteristic compatibility relations, Yu and Seebass[9] studied the same problem. For embedded shocks, they used a method similar to that of Hafez and Cheng.

Extension of the method of Hafez and Cheng to the full potential calculation is straightforward in principle; however, in practice, the more complicated coordinate systems used for the full potential calculations lead to cumbersome interpolation formulae.

In this paper we consider an alternative procedure for fitting shock waves in full potential calculations. (The application of the method to small disturbances is discussed in the Appendix.) The method is based on an equation for the unsteady shock jump, which is derived from the time-dependent equation describing the relaxation algorithm. In the steady-state limit, shock speed vanishes, and the steady shock polar is retained. In this way, the jump conditions are imposed iteratively and in a manner consistent with the relaxation procedure that is used everywhere else in the flow field. The method should be applicable to rotated difference schemes and to conservative and nonconservative differences.

The only previous work reported in literature on shock-fitting methods for full potential calculations is the work of Jones and South,[10] in which detached bow shock waves were considered. Jones and South first used a mapping from physical space to a rectangular computational grid; then, they used Newton's method to determine the shock shape. The method considered in this paper appears to be simpler and is not restricted to bow shocks.

In the following we first discuss unsteady transonic flow equations and their weak solutions. Then, the time-dependent equations describing the iterative methods are then developed. A shock-fitting algorithm is described, a solution procedure is proposed, and some preliminary numerical results are given. Finally, in the Appendix we compare the application of the shock-fitting algorithm to small-disturbance calculations with the method of Hafez and Cheng for one- and two-dimensional numerical examples.

2. Unsteady Full Potential Equations

For simplicity, we consider here the Cartesian coordinates x, y and t. The velocity potential ϕ is governed by

$$\phi_{tt} + 2u\phi_{xt} + 2v\phi_{yt} = (a^2 - u^2)\phi_{xx} - 2uv\phi_{xy} + (a^2 - v^2)\phi_{yy} \quad , \tag{1}$$

where

$$a^2 = \frac{1}{M_\infty^2} - \frac{\gamma - 1}{2}\left[2\phi_t + u^2 + v^2 - 1\right] ,$$

$$u = \phi_x + \cos\alpha \quad ,$$

$$v = \phi_y + \sin\alpha \quad ,$$

and α is the angle of attack of the oncoming flow with Mach number M_∞.

Equation (1) is not in conservative form. Multiplying by ρ/a^2, we obtain the conservative form

$$-\rho_t = (\rho u)_x + (\rho v)_y \quad , \tag{2}$$

where

$$\rho = \left[1 - \frac{\gamma - 1}{2} M_\infty^2 \left(2\phi_t + u^2 + v^2 - 1\right)\right]^{1/(\gamma - 1)} .$$

For smooth flows, equations (1) and (2) are equivalent. Equation (2), however, admits a weak solution with mass conservation across a discontinuity surface.

2.1 Jump Conditions

The jump condition admitted by the weak solution is given by

$$-S_t \left[\!\left[\rho \right]\!\right] = \left[\!\left[\rho u \right]\!\right] S_x + \left[\!\left[\rho v \right]\!\right] S_y \quad , \tag{3}$$

where $\left[\!\left[\rho \right]\!\right]$ denotes the jump in ρ across the surface

$$S(x,y,t) = 0 \quad .$$

In addition, from irrationality conditions we have

$$\phi_{tx} = \phi_{xt} \quad , \tag{4}$$

and $$\phi_{ty} = \phi_{yt} \quad .$$

Thus, $$S_t \left[\!\left[\phi_x \right]\!\right] = \left[\!\left[\phi_t \right]\!\right] S_x \quad ,$$

$$S_t \left[\!\left[\phi_y \right]\!\right] = \left[\!\left[\phi_t \right]\!\right] S_y \quad ,$$

or $$S_t : S_x : S_y = \left[\!\left[\phi_t \right]\!\right] : \left[\!\left[\phi_x \right]\!\right] : \left[\!\left[\phi_y \right]\!\right] \quad ,$$

which implies

$$\frac{d \left[\!\left[\phi \right]\!\right]}{dt} = \left[\!\left[\phi_t \right]\!\right] + \frac{dX}{dt} \left[\!\left[\phi_x \right]\!\right] + \frac{dy}{dt} \left[\!\left[\phi_y \right]\!\right] = 0 \quad ,$$

or $$\left[\!\left[\phi \right]\!\right] \equiv 0 \quad . \tag{5}$$

For steady states, equations (3) and (5) reduce to

$$\left[\!\left[\rho u \right]\!\right] - \frac{\partial X^D}{\partial y} \left[\!\left[\rho v \right]\!\right] = 0 \quad \text{or}$$

$$\left[\!\left[\rho \, q_n \right]\!\right] = 0 \quad ; \tag{6}$$

$$\left[\!\left[u \right]\!\right] \frac{\partial X^D}{\partial y} + \left[\!\left[v \right]\!\right] = 0 \quad \text{or} \quad \left[\!\left[q_s \right]\!\right] = 0 \quad , \tag{7}$$

where q_n is the relative normal velocity to the shock $X - X^D(y,t) = 0$, and q_s is the tangential velocity.

For transonic flows, equation (6) is a good approximation of Rankine Hugoniot relations*, the difference being due to the irrationality assumption.

*The exact Prandtl relation (taking into consideration entropy variations) may be used instead of eq. (6) in the manner suggested by Jones and South[10]; namely,

$$\left(q_n\right)_d \left(q_n\right)_u = a^{*2} - \frac{\gamma - 1}{\gamma + 1} q_s^2 \quad ,$$

where d and u refer to downstream and upstream conditions, and a^* is the sonic speed of sound.

2.2 Characteristics and Compatibility Relations

We note that equation (1) or (2) is always hyperbolic. (t is the time-like direction for both subsonic and supersonic flows.) Equation (1) can be written in the following form:

$$\phi_{tt} + 2q\phi_{st} = (a^2 - q^2)\phi_{ss} + a^2\phi_{nn} \quad , \tag{8}$$

where

$$\phi_{ss} = \frac{1}{q^2}\,(u^2\phi_{xx} + 2uv\phi_{xy} + v^2\phi_{yy}) \quad ,$$

$$\phi_{nn} = \frac{1}{q^2}\,(v^2\phi_{xx} - 2uv\phi_{xy} + u^2\phi_{yy}) \quad ,$$

$$\phi_{st} = \frac{u}{q}\,\phi_{xt} + \frac{v}{q}\,\phi_{yt} \quad ,$$

and q is the total velocity. Using the transformation $S = s - qt$, $N = n$, $T = t$, equation (8) reduces to: (freezing q , the coefficient of the ϕ_{st} term)

$$\phi_{TT} = a^2(\phi_{SS} + \phi_{NN}) \tag{9}$$

or, with the transformation $X = x - ut$, $Y = y - vt$, $T = t$, equation (1) reduces to

$$\phi_{TT} = a^2(\phi_{XX} + \phi_{YY}) \quad . \tag{10}$$

Equations (1) and (4) can be written as a system of first-order equations; namely

$$\begin{pmatrix} w \\ u \\ v \end{pmatrix}_t = \begin{pmatrix} -2u & a^2-u^2 & -uv \\ 1 & 0 & 0 \\ 0 & 0 & 0 \end{pmatrix} \begin{pmatrix} w \\ u \\ v \end{pmatrix}_x + \begin{pmatrix} -2v & -uv & a^2-v^2 \\ 0 & 0 & 0 \\ 1 & 0 & 0 \end{pmatrix} \begin{pmatrix} w \\ u \\ v \end{pmatrix}_y \quad ,$$

where

$$w = \phi_t \ , \quad a^2 = \frac{1}{M_\infty^2} - \frac{\gamma-1}{2} \ (2w + u^2 + v^2 - 1) \ . \tag{11}$$

For time-dependent problems, the characteristics and the compatibility relations are readily obtained from this system. For steady problems, they are given by

$$\left(\frac{dv}{du}\right)_{ch} = -\frac{A}{C}\left(\frac{dy}{dx}\right)_{ch} = -\frac{B \pm \sqrt{B^2-AC}}{C} \ , \tag{12}$$

where

$$A = a^2 - u^2$$
$$B = -uv$$
$$C = a^2 - v^2 \ .$$

3. Shock-Fitting Method

3.1 Iterative Solution for Steady Equation

It is well known that iterative line relaxation methods can be described by a time-dependent equation. For example, Jameson[7] showed that the convergence of the iterative solution of the full potential equation can be analyzed by

$$\alpha\phi_{xt} + \beta\phi_{yt} + \gamma\phi_{yyt} + \delta\phi_{t} = R_{NC}(\phi) \quad , \tag{13}$$

where $R_{NC}(\phi) = (a^2 - u^2)\phi_{xx} - 2uv\phi_{xy} + (a^2 - v^2)\phi_{yy}$.

Multiplying equation (9) by ρ/a^2 , we have

$$\bar{\alpha}\phi_{xt} - \bar{\beta}\phi_{yt} + \bar{\gamma}\phi_{yyt} + \bar{\delta}\phi_{t} = R_{Fc}(\phi) \quad , \tag{14}$$

where $$R_{Fc}(\phi) = (\rho u)_x + (\rho v)_y \quad .$$

Since we are interested only in the steady-state solution, the coefficients $\bar{\alpha}$, $\bar{\beta}$, $\bar{\gamma}$ and $\bar{\delta}$ may be selected to accelerate the convergence.

The jump conditions admitted by the weak solution of equation (10) (freezing the coefficients in the left-hand side) are given by

$$S_t \left[\!\left[\bar{\alpha}\phi_x + \bar{\beta}\phi_y + \bar{\gamma}\phi_{yy} \right]\!\right] = \left[\!\left[\rho u \right]\!\right] S_x + \left[\!\left[\rho v \right]\!\right] S_y \quad . \tag{15}$$

Let the shock surface $S(x,y,t)$ be described by the explicit relation $S = X - X^D(y;t) = 0$.

Hence,

$$\frac{\partial X^D}{\partial t} \left[\!\left[\bar{\rho} \right]\!\right] = \left[\!\left[\rho u \right]\!\right] - \frac{\partial X^D}{\partial y} \left[\!\left[\rho v \right]\!\right] \quad , \tag{16}$$

where $$\bar{\rho} = -(\bar{\alpha}\phi_x + \bar{\beta}\phi_y + \bar{\gamma}\phi_{yy}) \quad .$$

Equation (16) may be written in the form

$$A \frac{\partial X^D}{\partial t} + B \frac{\partial X^D}{\partial y} = C \quad , \tag{17}$$

where

$$A = [\![\, \bar{\rho} \,]\!] \quad ,$$

$$B = [\![\, \rho v \,]\!] \quad , \quad \text{and}$$

$$C = [\![\, \rho u \,]\!] \quad .$$

3.2 Shock-Fitting

Shock-fitting procedures similar to methods used for the unsteady Euler equations may be applied to the iterative calculations once the artificial time-dependent equation (17) describing the development of the solution through iteration is recognized. Since we are only interested in the steady-state solution, however, many simplifications may be made. Two cases are identified here.

3.2.1 Supersonic-Subsonic Shocks

Given an initial condition (an initial guess of the shock location $X^D(y;0)$ and a boundary condition (for example, $\partial X^D/\partial y\ (0,t) = 0$), equation (17) determines the new shock location $X^D(y;t)$ across which φ is continuous. Hence, a Dirichlet boundary condition is imposed on the subsonic (elliptic) flow downstream of the shock as shown in Sketch 1.

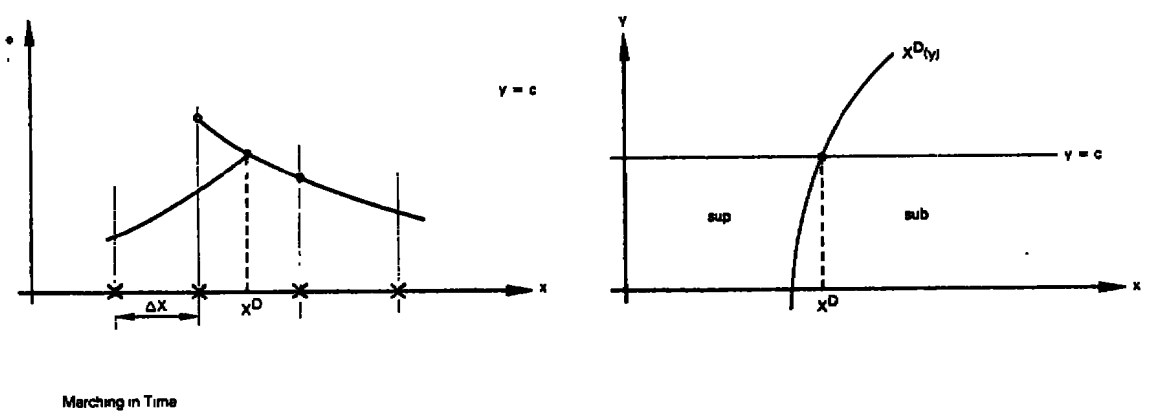

Sketch 1. Supersonic-Subsonic Shocks.

3.2.2 Supersonic-Supersonic Shocks

In general, the jump conditions and the characteristic compatibility relations admitted by the time-dependent equation uniquely determine the flow just downstream of the shock (ϕ and ϕ_n). Similar to the supersonic-subsonic shocks, equation (17) is used, and ϕ on the shock is obtained from upstream extrapolation. However, ϕ_n may be obtained by solving the compatability relations along the downstream characteristics together with the shock jump conditions (Equation 7), simultaneously to provide u and v downstream of the shock. These are needed for the supersonic flow calculations since, in rotated difference schemes, ϕ_{xx}, ϕ_{xy} and ϕ_{yy} terms contributing to ϕ_{ss} are backward differenced. Hence, the values of ϕ at two upstream grid points or equivalently the derivatives ϕ_x and ϕ_y are needed. We encountered some difficulties in implementing this scheme for supersonic-supersonic shocks in general. The details of a shock-fitting algorithm are discussed in the next section.

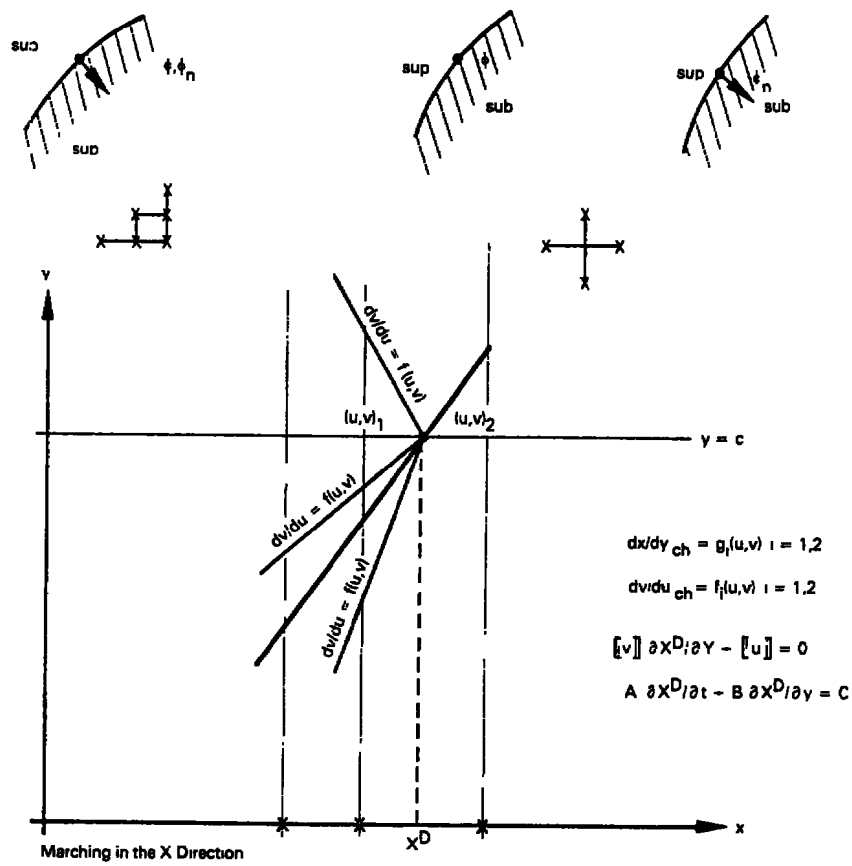

Sketch 2. Supersonic-Supersonic Shocks (Steady).

4. Numerical Implementation of Shock-Fitting Method

A shock-fitting algorithm has the following properties:

(1) An initial estimate of the potential is obtained, for example, from a nonconservative solution.

(2) The shock waves are detected and used as an initial estimate of shock location.

(3) The flow field is computed with a relaxation method, in which the shock is a surface of discontinuity fixed in space and the shock jump conditions are imposed as the boundary conditions.

(4) The shock locations are updated, based on the latest information, by using equation (17).

(5) Steps 3 and 4 are respected until convergence is achieved.

Step 1 requires no elaboration here. For step 2, different criteria may be used to detect a shock from smooth calculations. Murman[6] used the maximum slope point of the velocity profile in the shock region. South[11] used the minimum Laplacian ($\nabla^2\phi$) for full potential calculations. For supersonic-subsonic shocks, the shock points are suitable indicators of shock locations. Interpolation may be used between mesh points to locate the sonic velocity for a more accurate approximation. Jones and South[10] used an analytical form for the shock, with the right behavior in the far field (asymptotic to the Mach line) and near the axis (normal shock). To determine the standoff distance of a detached bow shock, Jones and South used the point with the same Mach number as the one downstream of a normal shock. Here we use a similar procedure, which is discussed in Section 5. For Step 4, the new shock location is obtained as a solution of equation (17). A Lax-Wendroff finite-difference scheme may be used to solve this equation. To avoid a stability restriction, we also tested an implicit scheme of the Crank-Nicholson type. A tridiagonal system is solved each time the shock is relocated. The finite-difference formula are

Lax-Wendroff Scheme:

$$X^{D^{n+1}} = X^{D^n} + \left(\frac{\partial X^D}{\partial t}\right)^n \Delta t + \left(\frac{\partial^2 X^D}{\partial t^2}\right)^n \frac{\Delta t^2}{2} \quad ,$$

$$\left(\frac{\partial X^D}{\partial t}\right)^n = -\frac{B}{A}\left(\frac{\partial X^D}{\partial y}\right)^n + \frac{C}{A}$$

$$\left(\frac{\partial^2 X^D}{\partial t^2}\right)^n = -\left(\frac{B}{A}\right) X^D_{yt} = -\frac{B}{A}\left[-\frac{B}{A}\left(\frac{\partial X^D}{\partial y}\right)^n + \frac{C}{A}\right]_y$$

Here we neglected the variation of A, B and C with time.

Crank-Nicholson Scheme:

$$X^{D^{n+1}} = X^{D^n} + 0.5\left[\left(\frac{\partial X^D}{\partial t}\right)^{n+1} + \left(\frac{\partial X^D}{\partial t}\right)^n\right]\Delta t \quad .$$

Once the shock is relocated, the continuity of ϕ is imposed as a boundary condition. For a detached bow shock, ϕ is set equal to zero, the free-stream value. For embedded shocks, the value of ϕ at the shock is obtained from upstream (supersonic) conditions by extrapolation. In the supersonic-subsonic case, to avoid use of a special unequal mesh formula at the grid point downstream of the shock, a Taylor series expansion is used to obtain a fictitious value of ϕ at the first mesh point upstream of the shock. This procedure is clearly demonstrated for the one-dimensional small-disturbance case in the appendix. It is used only for supersonic-subsonic shocks (i.e., if the flow downstream of the shock is subsonic) since it contradicts the rule of forbidden signals in the case of downstream supersonic flow. For the supersonic-supersonic shocks, two conditions ϕ and ϕ_n are needed to continue the calculation downstream of the shock. The value of ϕ on the shock is obtained from upstream extrapolation; ϕ_n can be obtained from studying equations 7 and 12 simultaneously. We have not succeeded in testing the scheme for supersonic-supersonic shocks.

5. Calculated Examples

We have obtained preliminary results for the flow past a blunt body by using the method of South and Jameson[12] with the above-described shock-fitting algorithm.* We use the Keller-South[14] (RAXBOD) program to obtain an initial estimate for ϕ everywhere in the flow field. The standoff distance is calculated as discussed earlier, and hyperbola is used as an initial estimate of the shock shape.

The shock is located by using equation (11). Properties ahead of the shock are calculated by extrapolation from upstream conditions; in this case, $\phi \equiv 0$ ahead of the shock. For the supersonic-supersonic part of the shock, we also need the properties behind the shock. Equations (7) and (12) provide ϕ_x and ϕ_y (hence ϕ_n) just downstream of the shock. In this example, we assume that ϕ_Y (i.e., the derivative of ϕ along the normal computational coordinate direction) just downstream of the shock is negligible. More accurate treatment for the supersonic-aupersonic shocks are meeded. Figure 1 shows the results for the pressure coefficient on the body calculated by the RAXBOD program for a sphere of radius one in a flow with $M_\infty = 1.2$. The physical plane is mapped to a rectangular grid (21 x 21 grid points), where

$$\eta = \frac{AY}{(1 - Y)^{\alpha}} , \alpha = 1.3 , \quad A = 1.25 \quad .$$

Here, η is the physical coordinate normal to the body, and Y is the computational coordinate, which varies from zero at the body to one at infinity. The tangential coordinate is stretched by a quadratic transformation between the physical arc length and the computational coordinate X .

*The same problem was solved by Jones and South,[10] who used mapping techniques, and by Hsieh[13] (hemisphere cylinder), who used the time-dependent Euler equation.

I	XB	YB	CP
1	.000	-.000	1.4137
2	.002	.065	1.4064
3	.013	.159	1.3799
4	.039	.276	1.2855
5	.088	.416	1.1324
6	.166	.552	.9050
7	.277	.691	.6119
8	.421	.815	.2810
9	.595	.914	-.0604
10	.791	.978	-.3704
11	1.000	1.000	-.6142
12	1.209	.978	-.7811
13	1.405	.914	-.8806
14	1.579	.815	-.9312
15	1.723	.691	-.9721
16	1.834	.552	-.9943
17	1.912	.410	.8553
18	1.961	.276	1.2074
19	1.987	.159	1.1487
20	1.998	.065	1.4028
21	2.000	.000	1.4137

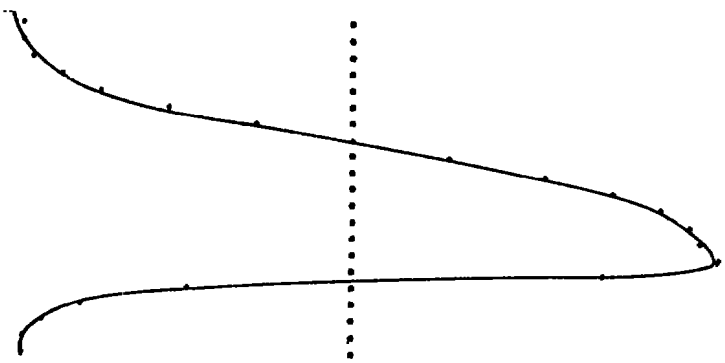

Figure 1. C_p on a Sphere at M = 1.2 (RAXBOD Solution).

Figure 2 shows the initial guess of the shock location. The movement of the shock (standoff distance) with iteration is plotted in Figure 3, and the final result is shown in Figure 4.

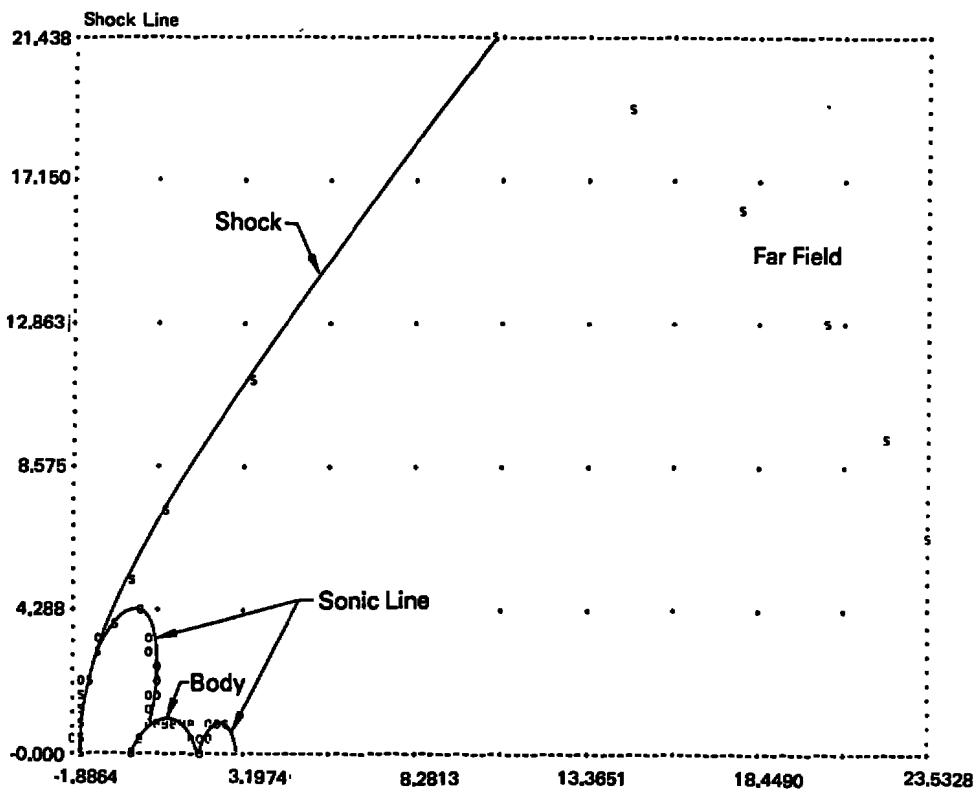

Figure 2. Initial Shock Location Detected From RAXBOD Solution.

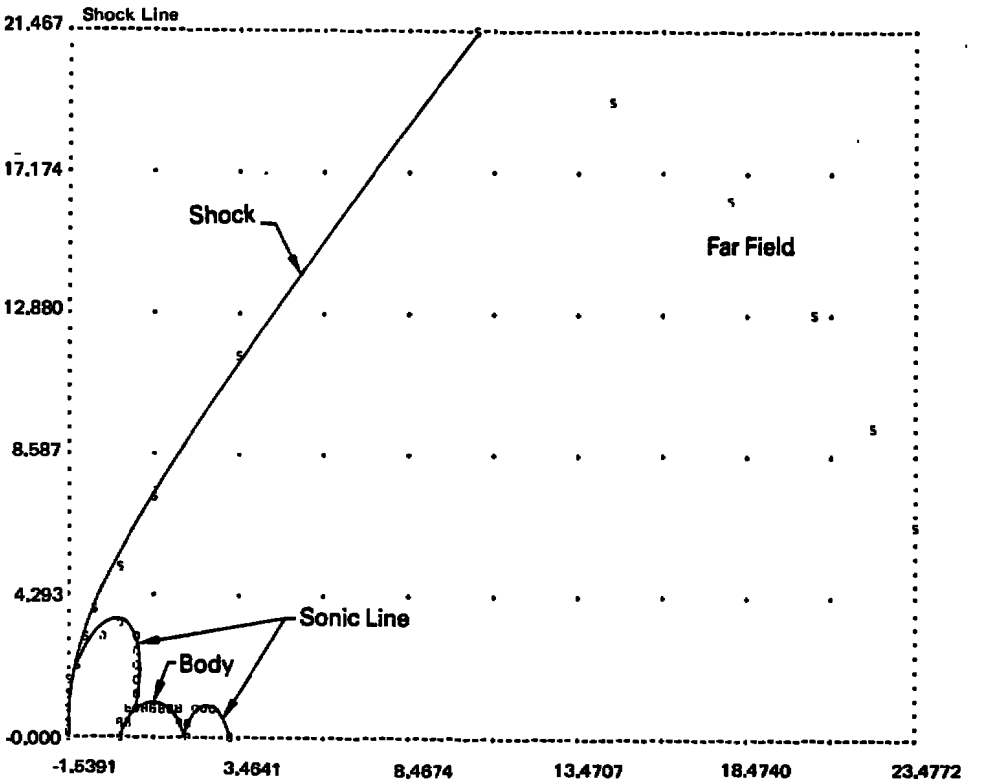

Figure 3. Movement of Shock During Iteration.

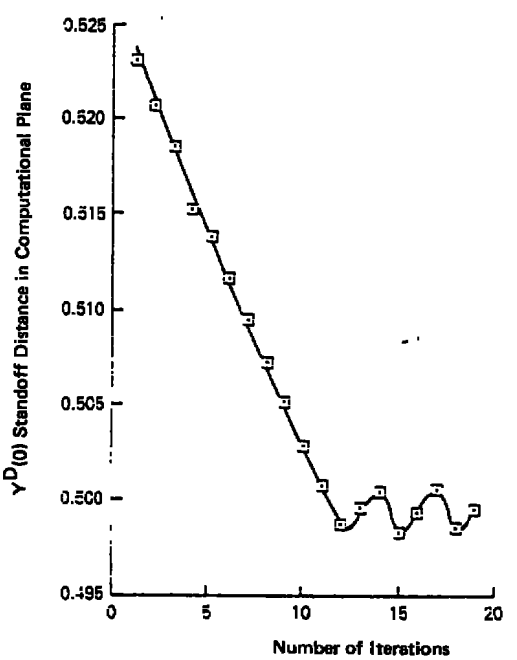

Figure 4. Shock Location After Shock Fitting.

It should be mentioned here that our results for the case of a sphere at $M_\infty = 1.2$ (based on the full potential calculations) indicate that the bow shock standoff distance differs by 20 percent from a time-dependent solution of Euler Equations given in Reference 13. These discrepancies cannot be traced to the difference between the Euler Equation and the full potential equation since in this range they should agree.

It could be argued that the discrepancies are due to the supersonic/ supersonic part of the shock where the shock was not really fitted in our calculation. This is unlikely, however, since the initial guess is selected using Moeckel's approximation. We have not resolved this point and further investigation is needed to resolve the differences.

Calculation of embedded shocks have been tested also. Flows around a sphere were computed with and without shock fitting. In Figure 5, results of the RAXBOD program are plotted. For the same mesh, results from the SAXBOD program are plotted in Figure 6. Notice that the overall pressure distribution does not seem to look different, however, the drag coefficient using Trapezoidal and Simpson's Rule are changed by about 20 percent. The same case has been calculated after a mesh refinement. The results of the RAXBOD program are shown in Figure 7, while the results of the SAXBOD program are shown in Figures 8 and 9.

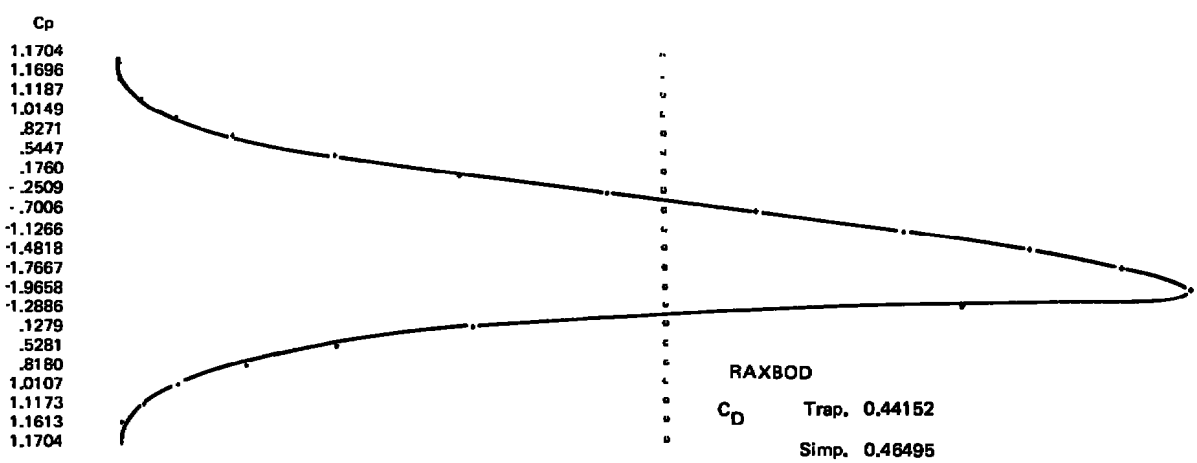

Figure 5. C_p on a Sphere at M = 1.2 (RAXBOD Solution).

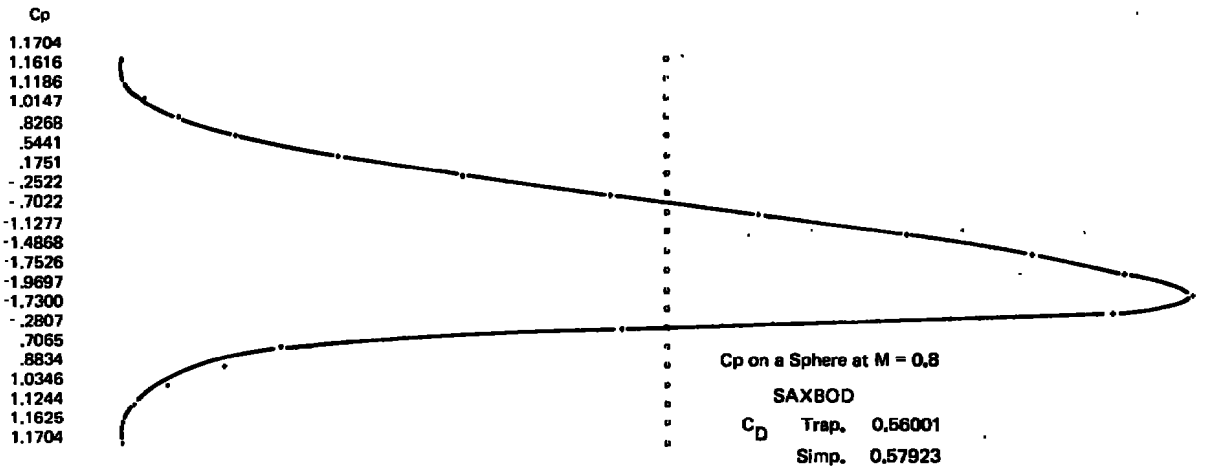

Figure 6. C_p on a Sphere at M = 1.2 (SAXBOD Solution).

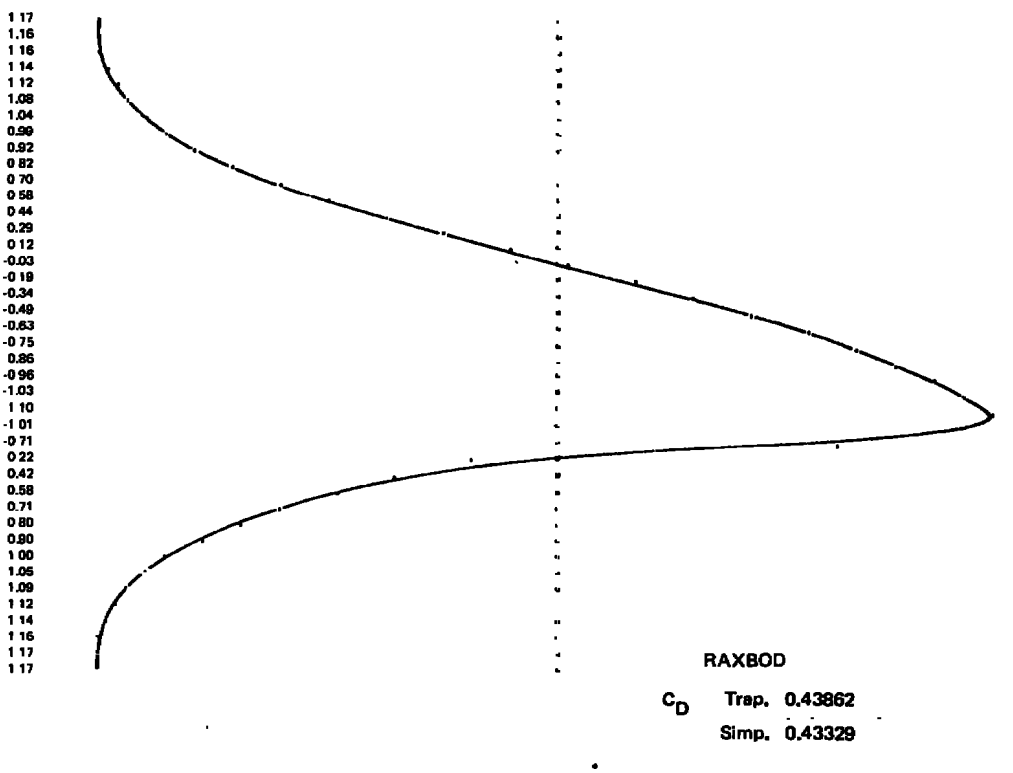

Figure 7. C_p on a Sphere at M = 1.2.

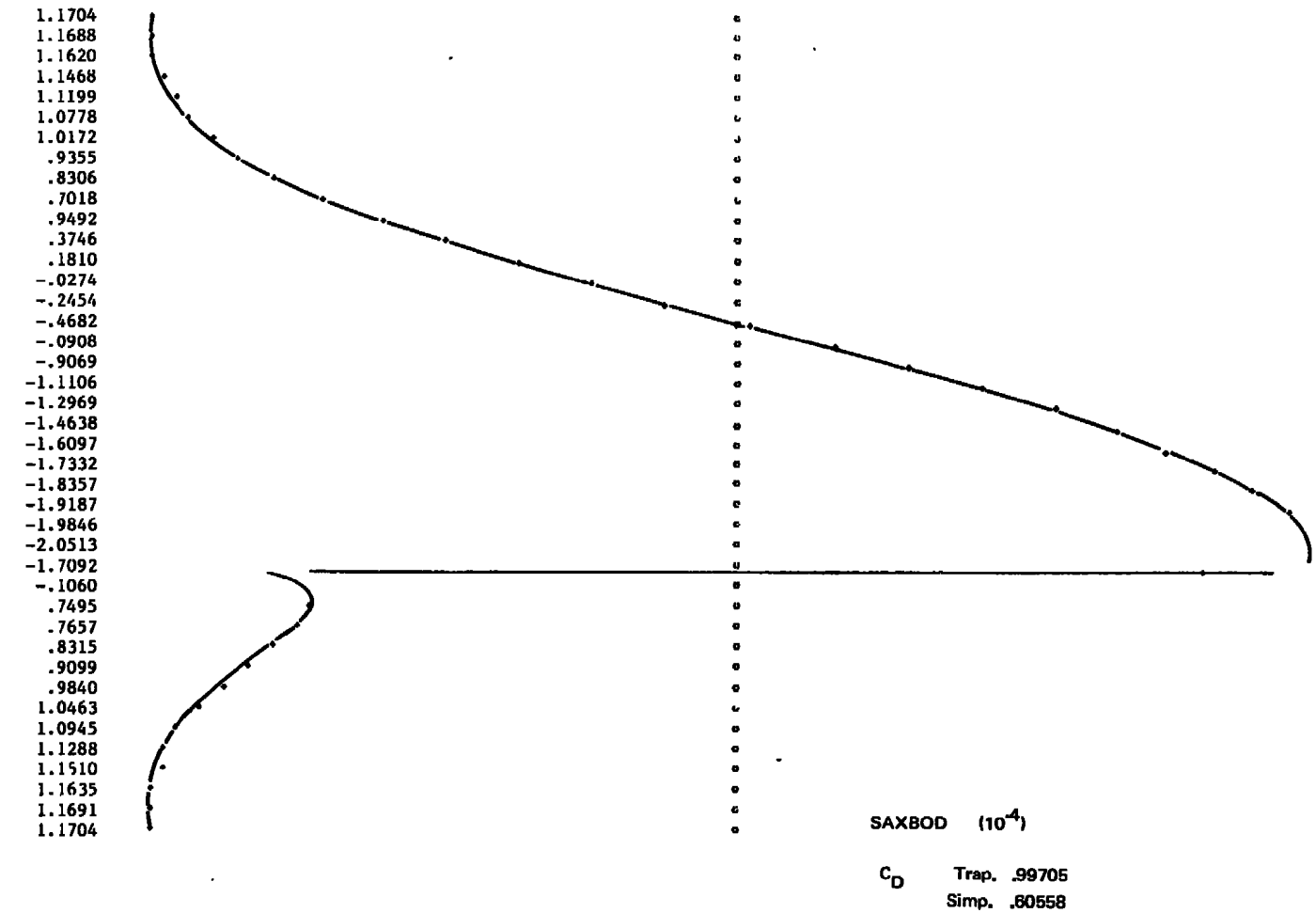

Figure 8. C_p on a Sphere at M = 1.2.

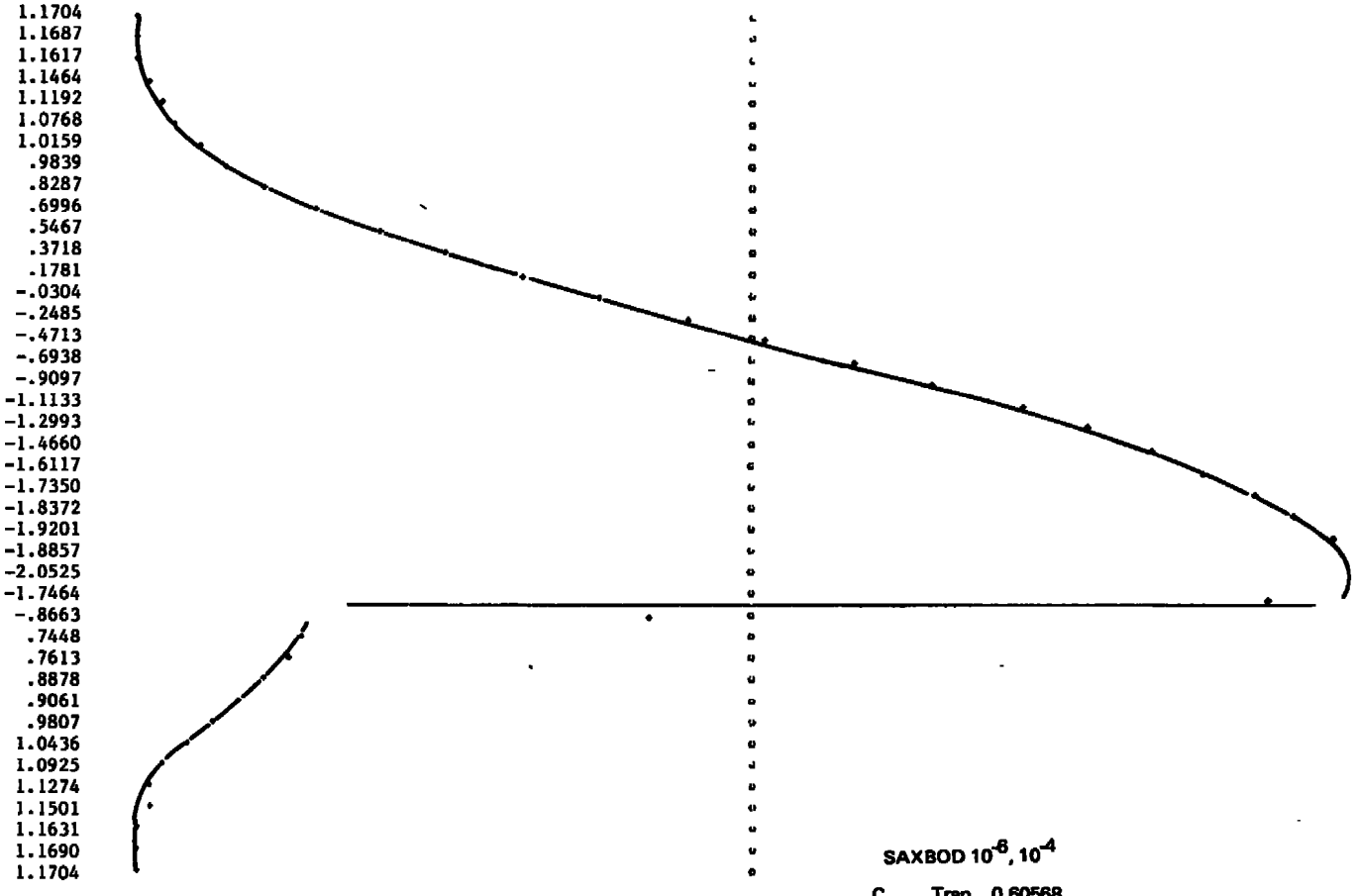

Figure 9. C_p on a Sphere at M = 1.2.

In the first case, the iterations were stopped when the maximum difference between successive iterates is less than 10^{-4} while more iterations were allowed (to 10^{-6}) for the results shown in Figure 5. The maximum residual (in the difference equation or the shock polar) is less than 10^{-3}. The difference in the pressure distribution is indistinguishable, but the drag coefficient shows 2 percent changes. Comparing RAXBOD and SAXBOD results, the drag coefficients are increased by mesh refinement when shock fitting is used, and decreased in the case of RAXBOD (nonconservative calculations). It would be interesting to run the same case using a conservative code. The computer listing of SAXBOD for embedded shocks are attached.

6. Conclusions

A shock-fitting algorithm for full potential type-dependent finite-difference relaxation calculations is described, and preliminary results are presented. The method is based on a time-dependent equation describing the line relaxation method. Written in conservative form, its weak solution admits an unsteady jump condition in terms of the shock speed. We use this equation to update the shock during the iterative calculations. Numerical implementations of the method are discussed, and the flow around a sphere is calculated. We have not succeeded in satisfactorily implementing the shock fitting algorithm for the supersonic-supersonic shock and more accurate treatment is needed. We also test this method for small-disturbance calculations.

Appendix

In this section, we consider the application of the proposed algorithm to the small-disturbance equation. The unsteady small-disturbance equations may be written as ($\beta = \alpha = 1$):

$$\beta M_\infty^2 \phi_{tt} + 2\alpha M_\infty^2 \phi_{xt} =$$

$$\left[(1 - M_\infty^2)\phi_x - \tfrac{1}{2}(\gamma + 1)M_\infty^2 \phi_x^2\right]_x + \phi_{yy} \tag{A.1}$$

$$\phi_{xt} = \phi_{tx}$$

$$\phi_{yt} = \phi_{ty} \quad .$$

Hence, the jump conditions admitted by the weak solution are

$$\left(M_\infty^2 \; [\![\phi_t]\!] + 2\alpha M_\infty^2 \; [\![\phi_x]\!]\right) S_t =$$

$$[\![(1 - M_\infty^2)\phi_x - \tfrac{1}{2}(\gamma + 1)M_\infty^2 \phi_x^2]\!] \; S_x + [\![\phi_y]\!] \; S_y$$

$$S_t \; [\![\phi_x]\!] = [\![\phi_t]\!] \; S_x$$

$$S_t \; [\![\phi_x]\!] = [\![\phi_t]\!] \; S_x \quad . \tag{A.2}$$

For $\beta = 0$, $\alpha = 1$, $S(x,y,t) = X - X^D(y,t) = 0$. We have*

$$2M_\infty^2 \frac{\partial X^D}{\partial t} = - \left\langle (1 - M_\infty^2) - (\gamma + 1)M_\infty^2 \phi_x \right\rangle + \left(\frac{\partial X^D}{\partial y}\right)^2 \tag{A.3}$$

$$- \frac{\partial X^D}{\partial t} \; [\![\phi_x]\!] = [\![\phi_t]\!] \; ,$$

$$- \frac{\partial X^D}{\partial t} \; [\![\phi_y]\!] = - [\![\phi_t]\!] \; \frac{\partial X^D}{\partial y} \quad .$$

*Equation (A.3) may be written in the equivalent (quasisteady) form:

$$[\![\left(1 - M_\infty^2\right) \phi_x - \frac{(\gamma + 1)}{2} M_\infty^2 \phi_x^2 - 2M_\infty^2 \phi_t]\!] - \frac{\partial X^D}{\partial y} \; [\![\phi_y]\!] = 0$$

For the steady state, equation (A.3) reduces to the shock polar

$$- \left\langle (1 - M_\infty^2) - (\gamma + 1)\, M_\infty^2 \phi_x \right\rangle = \left(\frac{\partial x}{\partial y}\right)^2_{\text{shock}} = \frac{[\![\phi_y]\!]^2}{[\![\phi_x]\!]^2} \qquad \text{(A.4)}$$

Equation (A.1) may be written as a system of first-order equations ($w = \phi_t$, $u = \phi_x$, $v = \phi_y$):

$$\beta w_t = \left[(1 - M_\infty^2)\, u - \tfrac{1}{2}(\gamma + 1)\, M_\infty^2 u^2\right]_x + v_y - \alpha 2 M_\infty^2 w_x$$

$$u_t = w_x$$

$$v_t = w_y \quad . \qquad \text{(A.5)}$$

Notice that, unlike the full potential case, the system of first-order equations is hyperbolic only if

$$\alpha^2 M_\infty^2 + 1 - M^2 > 0 \quad \text{where} \quad 1 - M^2 = 1 - M_\infty^2 - (\gamma + 1) M_\infty^2 \phi_x$$

The characteristics (and the compatibility relations) of the unsteady equations are obtained from this system (A.5). The steady-state relations are:

$$\left(\frac{dx}{dy}\right)^2_{\text{char.}} = \left(\frac{dv}{du}\right)^2_{\text{char.}} = (\gamma + 1)\, M_\infty^2\, u - (1 - M_\infty^2) \quad . \qquad \text{(A.6)}$$

We note that equation (A.4) simplifies to*

*Equation (A.6) is consistent with the weak shock approximation: The shock bisects the characteristics; in other words,

$$\left(\frac{dx}{dy}\right)_{\text{shock}} \Bigg/ \left[\left(\frac{dx}{dy}\right)^2_{\text{shock}} - 1\right] = \frac{\left\langle \left(\frac{dx}{dy}\right)_{\text{ch}} \right\rangle}{\left(\frac{dx}{dy}\right)_{u_{\text{ch}}} \left(\frac{dx}{dy}\right)_{u_{\text{ch}}} - 1} \quad .$$

$$\left\langle \left(\frac{dx}{dy}\right)^2_{char.} \right\rangle = \left(\frac{\partial x}{\partial y}\right)^2_{shock} \quad . \tag{A.7}$$

The development of solution during iteration may be described by

$$\alpha\phi_{xt} + \gamma\phi_{yyt} + \delta\phi_t =$$

$$\left[(1 - M_\infty^2)\phi_x - \frac{\gamma + 1}{2} M_\infty^2 \phi_x^2\right]_x + (\phi_y)_y \quad . \tag{A.8}$$

Hence, the shock is updated from the equation (for $\gamma = 0$)

$$A \frac{\partial x^D}{\partial t} + B \frac{\partial x^D}{\partial y} = C \quad , \tag{A.9}$$

where $A = \alpha$, $B = \frac{\partial x^D}{\partial y}$,

$$C = - \left\langle (1 - M_\infty^2) - (\gamma + 1) M_\infty^2 \phi_x \right\rangle .$$

One-Dimensional Example

Consider the following one-dimensional model equation for the unsteady problem

$$(\phi_x)_t + (\phi_x^2)_x = 0 \quad , \quad 0 \leq X \leq \ell \tag{A.10}$$

$$\phi(0,t) = 0 \quad , \quad \phi_x(0,t) = \phi_{x_L}$$

$$\phi(\ell,t) = 0$$

The jump condition is

$$\frac{\partial x^D}{\partial t} = \phi_{x_L} + \phi_{x_R} \quad . \tag{A.11}$$

We see that the speed of the shock is the average of the upstream and downstream velocities.**

** The governing equation is $u_t + 2uu_x = 0$; hence

$$\left(\frac{dx}{dt}\right)_{ch} = 2u \quad \text{and} \quad \left(\frac{dx}{dt}\right)_{sh} = \left\langle 2u_u + 2u_d \right\rangle \quad .$$

For $\ell = 2$ and $\phi_{x_L} = 1$, the steady-state solution is

$$\phi = X \qquad 0 \leq X \leq 1 \ ,$$

$$\phi = 2 - X \qquad 1 \leq X \leq 2 \ , \tag{A.12}$$

In Sketch A.1 we see that if we locate the shock incorrectly between zero and one the shock will move towards one. If the shock is placed at one, the shock speed is zero, and the shock settles there.

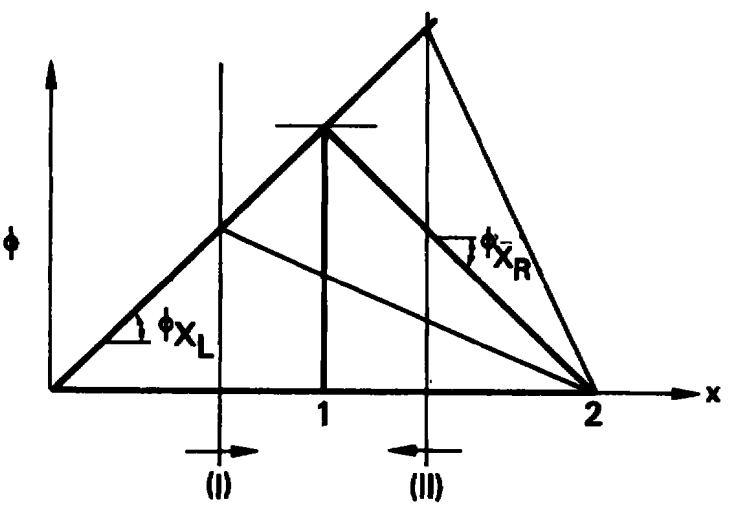

Sketch A.1

To check these ideas, we compared this method to that of Hafez and Cheng[8]. Hafez and Cheng considered the shock an internal boundary with a derivative (Neuman) boundary condition. Assuming that the initial guess of the shock location is at I, we can solve the flow downstream of the shock with a derivative boundary condition derived from the steady jump condition; in other words,

$$\phi_{x_R} = - \phi_{x_L} \tag{A.13}$$

The new position of the shock is determined by finding the intersection of the two ϕ solutions downstream and upstream of I, as demonstrated in in Sketch A.2.

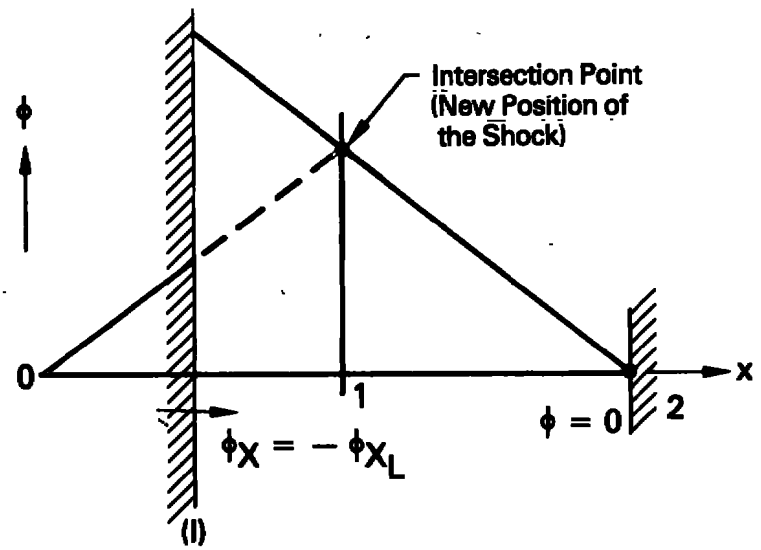

Sketch A.2

Sketch A.3 shows a case where the shock is placed incorrectly at II.

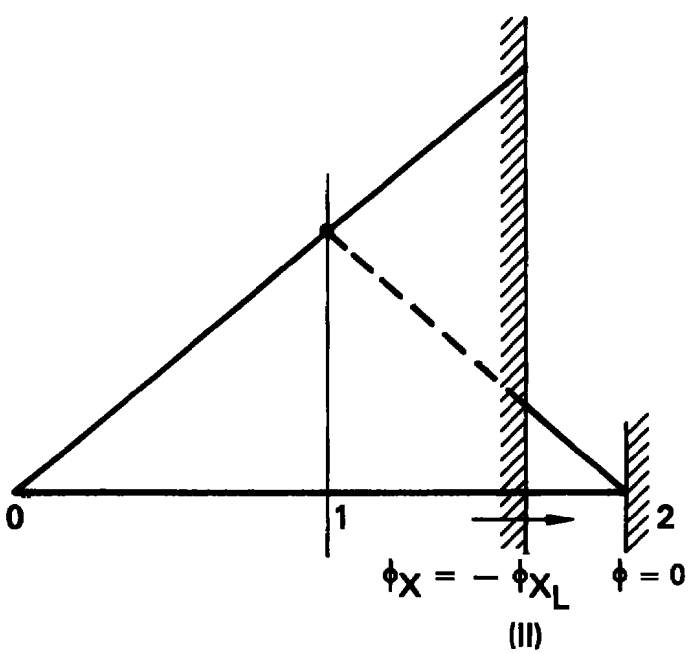

Sketch A.3

The continuity of ϕ across the shock (tangential velocities are the same) and the mass conservation condition switch roles in the two methods. Hafez and Cheng[8] used the mass conservation condition to calculate the flow downstream of the shock and the continuity of ϕ to determine the new shock location. In the present method we use the continuity of ϕ to calculate the flow downstream of the shock, and the shock moves to satisfy the mass conservation condition. Hafez and Cheng show that the results obtained with their method are identical to those obtained with Murman's fully conservative shock-point operator for the one-dimensional case. On the other hand, the present method uses the Dirichlet boundary condition to solve the flow downstream of the shock. Unlike the nonconservative calculations, mass is conserved by moving the shock to the correct place.

The finite-difference implementation of the Hafez and Cheng procedure for the one-dimensional problem considered here is

$$\frac{u_+^2 - u_-^2}{\Delta X} = 0 \quad , \tag{A.14}$$

where

$$u_+ = \frac{\phi_{i+1} - \phi_i}{\Delta X}$$

$$u_- = -\frac{\phi_{i-1} - \phi_{i-2}}{\Delta X} \quad ,$$

while the corresponding formula of the present method is (Sketch A.4)

$$\frac{u_+^2 - u_-^2}{\Delta X} = 0 \quad , \tag{A.15}$$

where

$$u_+ = \frac{\phi_{i+1} - \phi_i}{\Delta X} \quad ,$$

$$u_- = \frac{\phi_i - \phi_d}{\Delta X} \quad ,$$

$$\phi_d = \phi_{i-1} + (X^D - X_{i-1})$$

$$\times \left(\frac{\phi_{i-1} - \phi_{i-2}}{\Delta X} - \frac{\phi_{i+1} - \phi_i}{\Delta X} \right) \quad ,$$

and $$\frac{dX^D}{dt} = \frac{\phi_{i+1} - \phi_i}{\Delta X} + \frac{\phi_{i-1} - \phi_{i-2}}{\Delta X} \quad ,$$

which can be written in the form:

$$\frac{u_+^2 - u_-^2}{\Delta X} = C \quad , \tag{A.16}$$

where $u_+ = \frac{\phi_{i+1} - \phi_i}{\Delta X}$

$$u_- = \frac{\phi_i - \phi_{i-1}}{\Delta X}$$

$$\Delta X \cdot C = \left[\frac{\phi_{i-1} - \phi_d}{\Delta X}\right]^2 + 2\,\frac{\phi_{i-1} - \phi_d}{\Delta X}\,\frac{\phi_i - \phi_{i-1}}{\Delta X}$$

$$= \left[-\frac{X^D - X_{i-1}}{\Delta X}\left(\frac{\phi_{i-1} - \phi_{i-2}}{\Delta X} - \frac{\phi_{i+1} - \phi_i}{\Delta X}\right)\right]^2$$

$$- 2 \times \left[\frac{X^D - X_{i-1}}{\Delta X}\left(\frac{\phi_{i-1} - \phi_{i-2}}{\Delta X} - \frac{\phi_{i+1} - \phi_i}{\Delta X}\right)\right]\left(\frac{\phi_i - \phi_{i-1}}{\Delta X}\right) \quad .$$

Notice the left-hand side is the nonconservative difference scheme (elliptic operator) and the right-hand side is the correction (source) term needed to conserve mass.

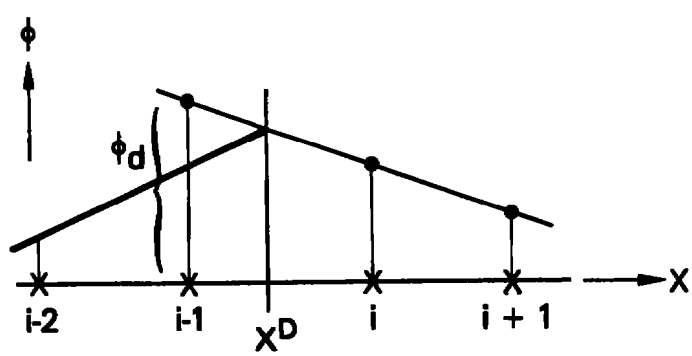

Sketch A.4

Two-Dimensional Examples

Supersonic-Subsonic Shocks.

In the method of Hafez and Cheng[8], an algebraic relation derived from a finite-difference approximation of the shock polar replaces the finite-difference approximation of the differential equation downstream of the shock; namely,*

$$\langle 1 - M_\infty^2 - (\gamma + 1)M_\infty^2\phi_x \rangle \frac{[\![\phi_x]\!]}{\Delta x} + \frac{[\![\phi_y]\!]}{\Delta y} = 0$$

where $$\beta = -\frac{\Delta y}{\Delta x}\frac{\partial x^D}{\partial y} = \frac{\Delta y}{\Delta x}\frac{[\![\phi_y]\!]}{[\![\phi x]\!]} ,$$

and where appropriate one-sided derivatives for ϕ_x and ϕ_y are used in the $[\![\ ]\!]$ and $\langle\ \rangle$ quantities. The shock is located at the intersection of the ϕ surfaces extrapolated from upstream and downstream calculations invoking the continuity of ϕ .

In the present method, an elliptic operator with a correction (source) term is used at the grid points just downstream of the shock. Fictitious points upstream of the shock similar to those in the one-dimensional case (as shown in Sketch A.5) are needed. The values of ϕ at these points (ϕ_{d1} , ϕ_{d2}) are obtained by extrapolation from the previous downstream solution and from the values of ϕ at the shock. The latter are obtained by extrapolation of the upstream solution to the shock position. The shock is then relocated by means of equation (A.9). Note that here we need the extrapolation procedures only to calculate a correction term. (An approximate location of the shock, for example, the middle of the mesh, may be used without great loss of accuracy.) Also, a locally normal shock-fitting approximation may be assumed (in other words, we may use the same formula as in the one-dimensional case, plus a centered difference approximation for the ϕ_{yy} term). As a matter of fact, Murman's fully conservative scheme may be written as an elliptic operator with a correction term, as follows:

*Murman's shock-point operator is a special case of this relation:

$$(\beta = 1 \quad \text{and} \quad [\![\ \phi_y\ ]\!]/\Delta y = (\phi_{yy})_{C.D.})$$

$$\left[(K\phi_x - \tfrac{1}{2}\phi_x^2)_x + \phi_{yy}\right]_{C.D.} = -\left[(K\phi_x - \tfrac{1}{2}\phi_x^2)_x\right]_{B.D.} .$$

All of these variants have been tested by modifying Murman's small-disturbance program. As shown in figure 10, we have calculated the flows around a 6% parabolic arc airfoil for a subsonic free stream ($M = 0.9$) by using

(i) Nonconservative scheme

(ii) Murman's fully conservative scheme

(iii) Fully conservative scheme in the form of an elliptic operator with a correction (source) term

(iv) Shock fitting (present method).

For these calculations, we used a 60 x 60 grid ($\Delta x = \Delta y = 0.05$), and the far field was set equal to zero. The convergence limit $|\phi^{n+1} - \phi^n| < 10^{-4}$ was usually reached in 50 iterations.

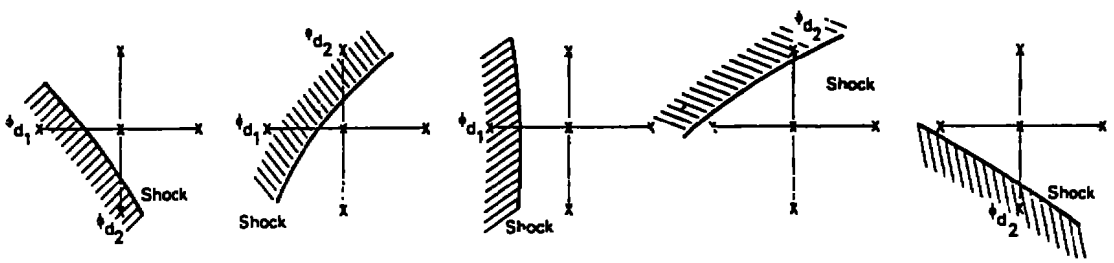

Sketch A.5

Supersonic-Supersonic Shocks.

For supersonic-supersonic shocks, Hafez and Cheng[8] used equation (A.7) to locate the shock in a step-by-step procedure. With the present method, we solve the problem iteratively where the shock moves according to equation (A.9). The value of ϕ at the shock is used as a boundary condition for the unknown on a vertical line between the shock location and the body (axis). Since background differences are used, values along the i-1 and i-2 lines are needed. Extrapolation in the Y direction is used to obtain the values of ϕ for those points upstream of the shock. As shown in figure 11, we have calculated the flows around a 6% parabolic arc airfoil for a supersonic stream ($M_\infty = 1.15$) by using

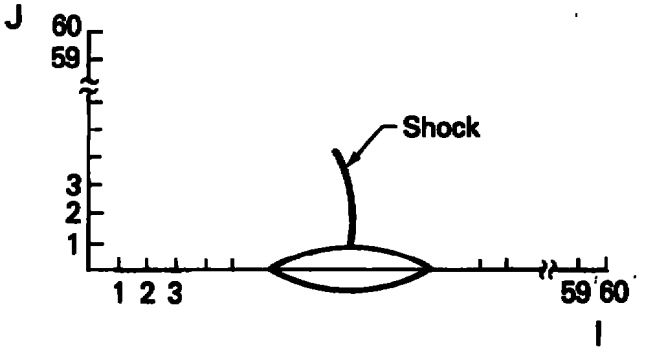

Figure 10. Supersonic-Subsonic Shocks.

J							SONIC LINE COORDINATES J	Y	XSONIC		XSH(J)
17	32	33	34	35			1	0.00000	.28155	.86573	.86573
16	32	33	34	35			2	.05000	.30077	.86228	.86228
15	32	33	34	35			3	.10000	.31803	.79820	.79820
14	32	33	34	35	36		4	.15000	.33535	.79440	.79440
13	32	33	34	35	36		5	.20000	.35273	.79071	.79071
12	32	33	34	35	36		6	.25000	.36907	.78656	.78656
11	32	33	34	35	36		7	.30000	.38662	.78257	.78257
10	32	33	34	35	36		8	.35000	.40420	.77846	.77846
9	32	33	34	35	36		9	.40000	.42067	.77254	.77254
8	32	33	34	35	36	37	10	.45000	.43885	.76641	.76641
7	32	33	34	35	36	37	11	.50000	.45700	.75850	.75850
6	32	33	34	35	36	37	12	.55000	.47460	.75047	.75047
5	32	33	34	35	36	37	13	.60000	.49506	.74107	.74107
4	32	33	34	35	36	37	14	.65000	.51548	.73056	.73056
3	32	33	34	35	36	37	15	.70000	.53952	.71450	.71450
2	32	33	34	35	36	37	16	.75000	.56400	.69584	.69584
1	32	33	34	35	36	37	17	.80000	.60225	.67628	.67628

Figure 10(a). Nonconservative Calculations.

J								SONIC LINE COORDINATES J	Y	XSONIC		XSH(J)
19	32	33	34	35				1	0.00000	.28066	.86503	.86503
18	32	33	34	35	36			2	.05000	.29949	.86228	.86228
17	32	33	34	35	36			3	.10000	.31699	.85976	.85976
16	32	33	34	35	36	37		4	.15000	.33455	.85712	.85712
15	32	33	34	35	36	37		5	.20000	.35181	.85416	.85416
14	32	33	34	35	36	37		6	.25000	.36827	.85075	.85075
13	32	33	34	35	36	37		7	.30000	.38496	.84680	.84680
12	32	33	34	35	36	37		8	.35000	.40213	.84223	.84223
11	32	33	34	35	36	37		9	.40000	.41832	.83698	.83698
10	32	33	34	35	36	37	38	10	.45000	.43547	.83098	.83098
9	32	33	34	35	36	37	38	11	.50000	.45288	.82426	.82426
8	32	33	34	35	36	37	38	12	.55000	.47014	.81641	.81641
7	32	33	34	35	36	37	38	13	.60000	.48879	.80835	.80835
6	32	33	34	35	36	37	38	14	.65000	.50780	.79955	.79955
5	32	33	34	35	36	37	38	15	.70000	.52735	.78968	.78968
4	32	33	34	35	36	37	38	16	.75000	.54916	.77842	.77842
3	32	33	34	35	36	37	38	17	.80000	.57172	.75984	.75984
2	32	33	34	35	36	37	38	18	.85000	.60008	.74058	.74058
1	32	33	34	35	36	37	38	19	.90000	.63896	.70769	.70769

Figure 10(b). Fully Conservative Calculations.

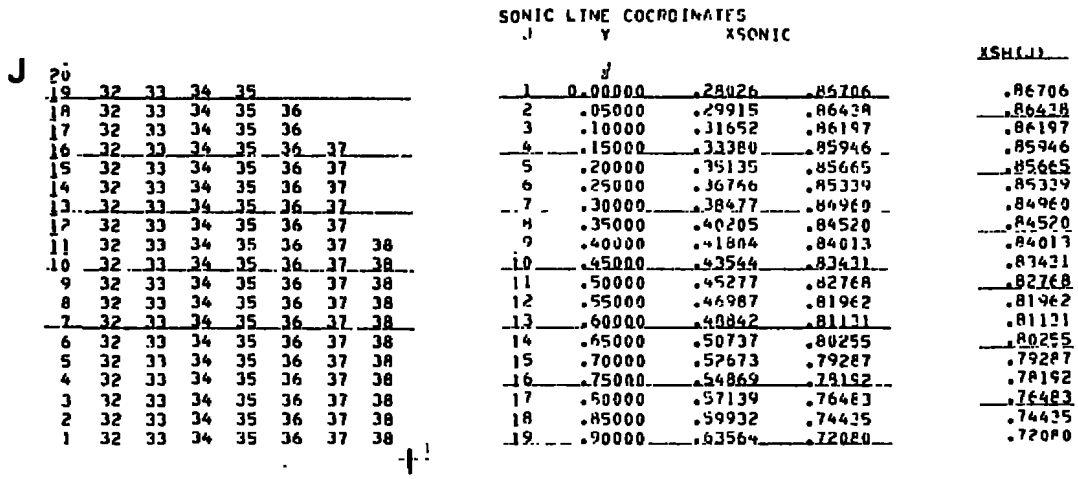

SONIC LINE COORDINATES

J	Y	XSONIC		XSH(J)
1	0.00000	.28026	.86706	.86706
2	.05000	.29915	.86438	.86438
3	.10000	.31652	.86197	.86197
4	.15000	.33380	.85946	.85946
5	.20000	.35135	.85665	.85665
6	.25000	.36746	.85339	.85339
7	.30000	.38477	.84960	.84960
8	.35000	.40205	.84520	.84520
9	.40000	.41804	.84013	.84013
10	.45000	.43544	.83431	.83431
11	.50000	.45277	.82768	.82768
12	.55000	.46987	.81962	.81962
13	.60000	.48842	.81131	.81131
14	.65000	.50737	.80255	.80255
15	.70000	.52673	.79287	.79287
16	.75000	.54869	.78192	.78192
17	.80000	.57139	.76483	.76483
18	.85000	.59932	.74435	.74435
19	.90000	.63564	.72080	.72080

J: 20 19 18 17 16 15 14 13 12 11 10 9 8 7 6 5 4 3 2 1 — 32 33 34 35 36 37 38

Figure 10(c). Modified Shock Point Operator Results (Elliptic Operator With a Correction Term).

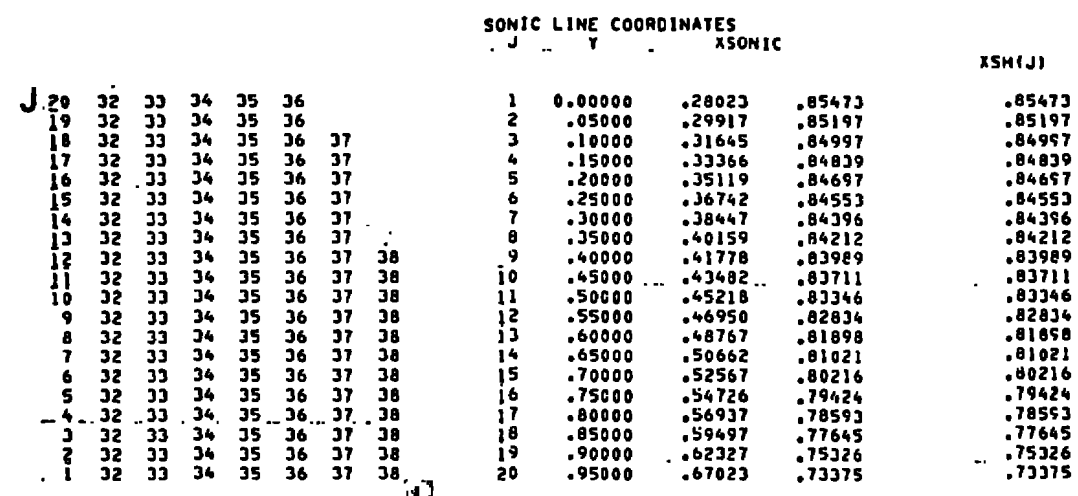

SONIC LINE COORDINATES

J	Y	XSONIC		XSH(J)
1	0.00000	.28023	.85473	.85473
2	.05000	.29917	.85197	.85197
3	.10000	.31645	.84997	.84997
4	.15000	.33366	.84839	.84839
5	.20000	.35119	.84697	.84697
6	.25000	.36742	.84553	.84553
7	.30000	.38447	.84396	.84396
8	.35000	.40159	.84212	.84212
9	.40000	.41778	.83989	.83989
10	.45000	.43482	.83711	.83711
11	.50000	.45218	.83346	.83346
12	.55000	.46950	.82834	.82834
13	.60000	.48767	.81898	.81898
14	.65000	.50662	.81021	.81021
15	.70000	.52567	.80216	.80216
16	.75000	.54726	.79424	.79424
17	.80000	.56937	.78593	.78593
18	.85000	.59497	.77645	.77645
19	.90000	.62327	.75326	.75326
20	.95000	.67023	.73375	.73375

J: 20 19 18 17 16 15 14 13 12 11 10 9 8 7 6 5 4 3 2 1 — 32 33 34 35 36 37 38

Figure 10(d). Shock-Fitting Results.

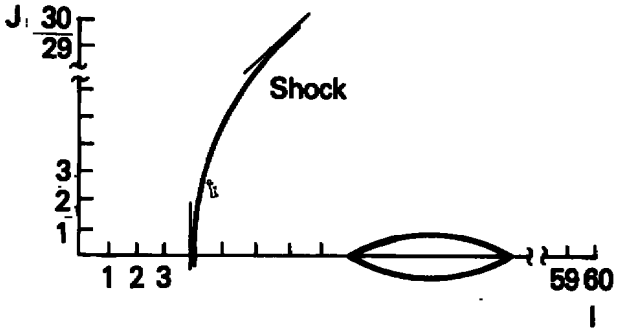

Figure 11. Supersonic-Supersonic Shocks

SONIC LINE COORDINATES

J	Y		XSONIC
1	0.00000	-.27367	.21552
2	.10000	-.27279	.24613
3	.20000	-.27014	.27072
4	.30000	-.26557	.29050
5	.40000	-.25859	.31508
6	.50000	-.24752	.33533
7	.60000	-.23175	.35234
8	.70000	-.21030	.36483
9	.80000	-.18986	.37312
10	.90000	-.16630	.38343
11	1.00000	-.14307	.39651
12	1.10000	-.11717	.40931
13	1.20000	-.09201	.41759
14	1.30000	-.06298	.42088
15	1.40000	-.03319	.42112
16	1.50000	.00338	.42115
17	1.60000	.03442	.42232
18	1.70000	.06766	.42368
19	1.80000	.10083	.42386
20	1.90000	.12260	.42171
21	2.00000	.16855	.19175
22	2.10000	.24949	.41005
23	2.20000	.30005	.39675
24	2.30000	.35820	.38361

Figure 11(a). Nonconservative Calculations (Did Not Converge in 200 Iterations).

SONIC LINE COORDINATES

J	Y		XSONIC
1	0.00000	-.12460	.20530
2	.10000	-.11615	.23445
3	.20000	-.09985	.25976
4	.30000	-.07985	.28256
5	.40000	-.05246	.30410
6	.50000	-.02705	.32279
7	.60000	.00573	.34211
8	.70000	.03904	.35954
9	.80000	.07022	.37659
10	.90000	.10850	.39318
11	1.00000	.14712	.40804
12	1.10000	.18360	.42306
13	1.20000	.22068	.43949
14	1.30000	.26397	.45455
15	1.40000	.30873	.46981
16	1.50000	.35415	.48197
17	1.60000	.40215	.49834
18	1.70000	.45713	.51035

Figure 11(b). Fully Conservative Calculations.

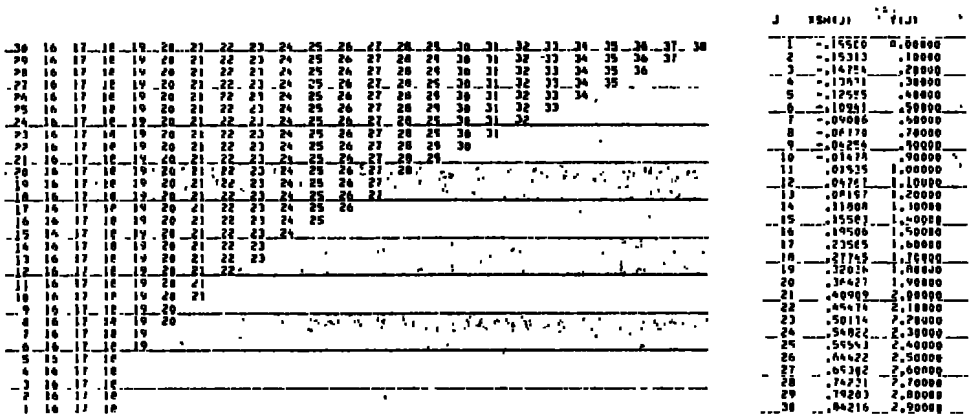

Figure 11(d). Shock-Fitting Results.

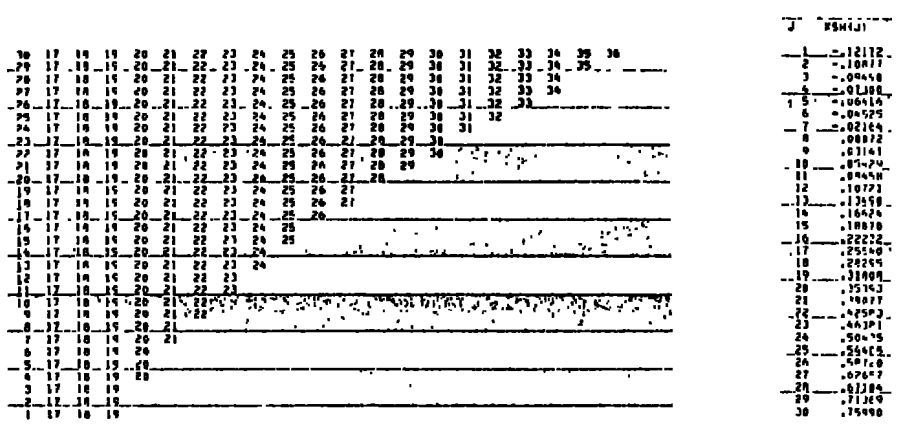

Figure 11(c). Initial Shock Location Predicted From Nonconservative Calculations.

(i) Nonconservative scheme

(ii) Fully conservative scheme

(iii) Shock fitting (present method);

For the calculations shown in figure 11, we used a 60 x 30 grid ($\Delta x = 0.05$, $\Delta y = 0.1$).

REFERENCES

1. Magnus, R. and Yoshihara, H., "Inviscid Transonic Flow Over Airfoils," AIAA J. 8, No. 2, 2157-2161, December, 1970.

2. Grossman, B. and Moretti, G., "Time-Dependent Computation of Transonic Flows," AIAA Paper, Houston, Texas, 70-1322, 1970.

3. Kentzer, C., "Discretization of Boundary Conditions on Moving Discontinuities," Proceedings of the Second International Conference on Numerical Methods in Fluid Mechanics, Lecture Notes in Physics (Vol. 8), Springer-Verlag, New York, 1971.

4. Murman, E. M. and Cole, J., "Calculation of Plane Steady Transonic Flow," AIAA J. 9, No. 1, 114-121, 1971.

5. Jameson, A., "Iterative Solution of Transonic Flows Over Airfoils and Wings," Comm. Pure Appl. Math 27, 283-309, 1974.

6. Murman, E. M., "Analysis of Embedded Shock Waves Calculated by Relaxation Methods," AIAA J. 12, No. 5, 626-633, 1973.

7. Jameson, A., "Transonic Potential Flow Calculation Using Conservation Form," Proceedings of the AIAA Third Computational Fluid Dynamics Conference, Hartford, Connecticut, June, 1975.

8. Hafez, M. and Cheng, H. K., "Shock Fitting Applied to Relaxation Solutions of Transonic Small Disturbance Equations," AIAA J., June, 1977.

9. Yu, N. J. and Seebass, A. R., "Second Order Numerical Solutions of Transonic Flows Over Airfoils With and Without Shock Fitting," Symposium Transsonicum II, Gotingen, September, 1975.

10. Jones, D. J. and South, J. C., "A Numerical Determination of the Bow Shock Wave in Transonic Axisymmetric Flow About Blunt Bodies," National Research Council Canada Report LR-586, Ottawa, 1975.

11. South, J. C., private communication, 1977.

12. South, J. C. and Jameson, A., "Relaxation Solutions for Inviscid Axisymmetric Transonic Flow Over Blunt or Pointed Bodies," AIAA Computational Fluid Dynamics Conference, Palm Springs, California, 1973.

13. Hsieh, T., "Flow Field Study About a Hemispherical Cylinder in Transonic and Low Supersonic Mach Number Range," AIAA Paper 75-83, 1975.

14. Keller, J. D. and South, J. C., "RAXBOD: A Fortran Program for Inviscid Transonic Flow Over Axisymmetric Bodies," NASA TM X-72, 331, 1976.